Original Article

Evaluation of Corona Charge Positive and Negative Impulses on Polymeric Surfaces and Simulation of Impact Rate

Ebadollah Amouzad Mahdiraji*

Department of Engineering, Sari Branch, Islamic Azad University, Sari, Iran

Use your device to scan and read the article online

Citation E. Amouzad Mahdiraji, **Evaluation of Corona Charge Positive and Negative Impulses on Polymeric Surfaces and Simulation of Impact Rate.** *Eurasian J. Sci. Technol.,* **2021**, *1*(4), 223-230.

https://doi.org/10.48309/EJST.2021.289237.1038

Article info:
Received: 04 April 2021
Accepted: 14 June 2021
Available Online: 14 June 2021
ID: JSTR-2106-1038
Checked for Plagiarism: Yes
Checked by Language Editor: Yes

Keywords:
Charging Radius, Glow Corona, Burst Impulse Corona, Polymeric Analisis, Transitional Mode.

ABSTRACT

Corona electric discharge phenomenon occurs when the electric field intensity exceeds the corona threshold. In the analysis of this paper, three types of hypotheses of partial charge, i.e. electrons, positive ions, and negative ions, generated in the air due to corona electrical discharge are considered. The physical process is produced along with the changes and dynamics of the electric charge applied to the field by the charge movement which has velocity due to electric fields and motion due to slope (diffusion). We will also see losses in electric charge. In this paper, electric load evaluation on a polymer surface by a positive impact corona in the air was performed. Output (circuit current) and input (electric fields and electric charge space density) are considered in computer simulation analysis. Different models have been used to identify the corona, depending on the intensity and extent of the voltage surges. The dynamics and distribution of electric charges and electric fields are analyzed and compared by two models of corona charging, i.e. glow and burst impulse).

Introduction

AlthoBy creating a leakage current between the two electrodes, the corona can cause more current to be drawn from the source, resulting in power losses. Corona produces ozone gas, and because ozone is a toxic gas, it can be harmful and dangerous. This gas is harmful even to a small extent to people with asthma. The Damages caused by corona include the accumulation of nitric acid and the formation of hair-shaped seams in insulating materials. Corona can be defined as local discharges that inductive effects of the corona phenomenon can also be problematic. Voltage induction can cause electric shocks and cause problems for humans. Corona produces a variety of noises, including audio noise, radio noise, and television noise. If the distance between the conductors is short, the corona may ignite and short circuit. It is obvious that corona causes loss of electrical energy and reduces the electrical efficiency of transmission lines.

are the result of strong, non-uniform electric fields and can lead to the deterioration of the insulator and sometimes its complete collapse [1-15]. The corona also has advantages, the

*Corresponding Author: Ebadollah Amouzad Mahdiraji (ebad.amouzad@gmail.com)

most important of which is that it acts like a safety valve when severe lightning strikes power lines, and the excess voltage caused by the lightning is lost in the form of corona losses. Therefore, most line voltages are designed to be close to the critical corona voltage so that the corona is formed immediately by lightning [16-27]. This is important because corona phenomena are often overlooked in electromagnetic transient helical analysis or as a phenomenon that negatively affects power systems. But in this study, we intend to evaluate the positive effects of corona on lightning strikes in the power system and show that the corona plays an important role in improving the reduction of the overvoltage range of lightning and improving the BIL size of transmission lines [18-30]. Increasing the conductor radius due to the corona reduces the wave of internal impedances and the wave of reciprocal impedances around the conductor remains unchanged. It also increases the capacitance and conduction of the ground line and increases the coupling coefficient around the conductors. But the conductor inductance parameters remain unchanged [28-30]. Different frequency parameters of the transmission line have relatively large effects on the transient state of electromagnetism under lightning strikes. Therefore, in this paper, according to the JMarti line model, different frequency parameters are considered. This model uses the linear impedance function of the line to provide a circuit equivalent to electrical transmission lines [31-35].

This paper attempts to make an electric evaluation of the polymer surface by a positive and negative impact corona in the air. Output (circuit current) and input (electric fields and electric charge space density) are considered in computer simulation analysis [36-39]. Different models have been used to identify the corona, depending on the intensity and extent of the voltage surges. The dynamics and distribution of electric charges and electric fields are analyzed and compared by two models of corona charging, i.e., glow and burst impulse.

Electrical Discharge Calculations

In the analysis of this paper, three types of hypotheses of partial charge, i.e., electrons, positive ions, negative ions, generated in the air due to corona electrical discharge are considered. The physical process is produced along with the changes and dynamics of the electric charge applied to the field by the charge movement which has velocity due to electric fields (thrust) and motion due to slope (diffusion) and we will also see losses in electric charge [39-41]. This phenomenon is modeled using continuous equations for each electric charge carrier and Poisson equations for the electric potential as follows:

(1) $$\partial n_e / \partial t + \nabla(-n_e \mu_e E - D_e \nabla n_e) = S_e$$

(2) $$\partial n_p / \partial t + \nabla(n_p \mu_p E - D_p \nabla n_p) = S_p$$

(3) $$\partial n_n / \partial t + \nabla(-n_n \mu_n E - D_n \nabla n_n) = S_n$$

$$\nabla(\varepsilon_0 \nabla \phi) = -q(n_p - n_e - n_n)$$

(4) $$E = -\nabla \phi$$

Where n is the constant charge density of the carrier D, emission coefficient, μ indicates mobility, E is the electric field vector, ∅ is the electric potential, S is the rate of plasma electric discharge processes, C is the initial charge, ε0 is the vacuum electrical conductivity and e, p, n is respectively Represent negative ions, positive ions, electrons. The number of losses and electric production are calculated according to the listed coefficients as follows:

(5)

$$S_e = \alpha n_e |w_e| - \eta n_e |w_e| - R_{ei} n_e n_p + \nu_{\det} n_n + S_0$$

$$S_p = \alpha n_e |w_e| - R_{ei} n_e n_p - R_{ii} n_p n_n + S_0$$

$$S_n = \eta n_e |w_e| - R_{ii} n_p n_n - \nu_{\det} n_n$$

Figure 1 shows the results of the computational field. This model is implemented in the COMSOL package based on the finite element method.

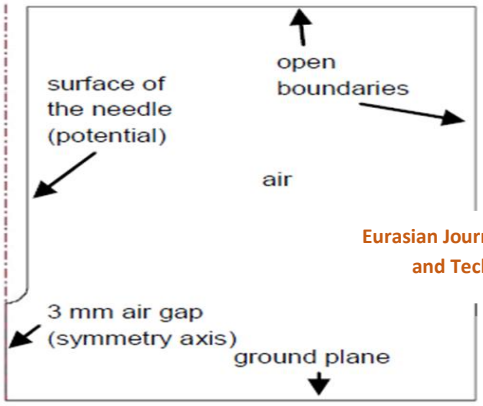

Figure 1 Computational field

This model has been developed by numerous comparisons of current circuit output waveforms with experimental results obtained from positive impact corona. The experimental startup diagram is shown in figure (2). The 0.95mm needle electrode is located 5mm from the electrode surface and is connected to a high voltage impulse generator.

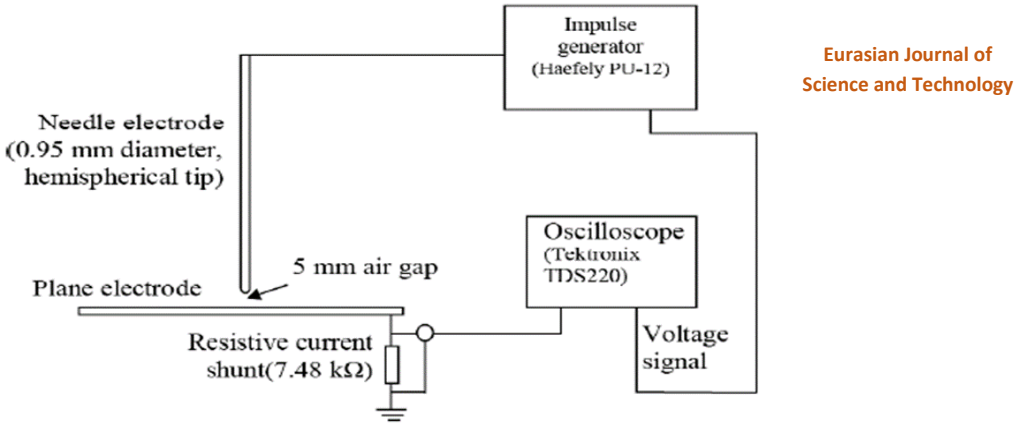

Figure 2 Experimental setup

By applying voltage, measurements and calculations of the current waveform obtained with 3kv with a switching stroke of 250/2500μs are shown in figure (3). One of the observations at the highest current value is the zero-voltage shock time, and when the current value is zero, the voltage shock is at its peak, and after the current is negative at 500 s, the shock intensity decreases.

Figure 4 shows the applied voltage, the total current measured and calculated, and the alternating current calculated according to the 6kv switching impulse.

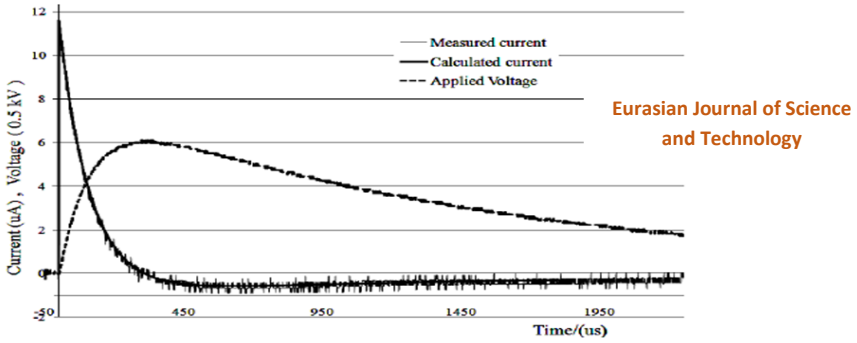

Figure 3 Current calculated and measured with switching impulse and actual voltage of 3kv

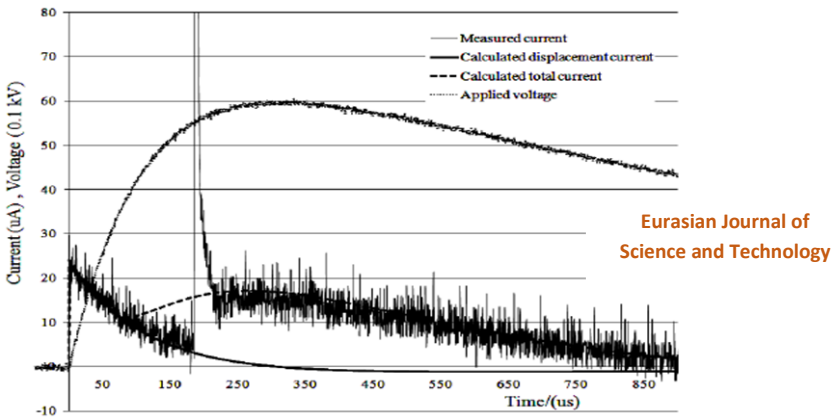

Figure 4 Current calculated and measured by switching impulse and actual voltage 6kv

Glow Corona

In the proposed system, the characteristics of the electric discharge of the corona are determined by the electric behavior of the space in the diffusion zone. The main part of the distance, which includes the positive charge of the space, is shown in figure (5). The maximum concentration of positive ions is reached at a distance of 0.15 from the anode. The concentration of ions increases in the forehead of the applied blows and the concentration of positive ions decreases at the end of the applied blows. Figure (6) shows the difference between the total current calculated and the alternating current with time with the same applied voltage shocks. At t = 0-100 and t> 1400 shows the total current and at t = 100-1400μs shows the alternating part which has a capacitive state. t ~ 100μs is the corona threshold, and with the application of voltage, the current reaches its maximum at t ~ 300μs. Figure (7) shows the difference between the actual electric field (taking into account the effect of the charging space) and the Laplace electric field (excluding the charging space) at the needle electrode. Observations show that the duration of electric discharge occurs at t = 100-1400μs and the intensity of the real electric field is less than the intensity of the Laplace electric field and the level of the real electric field remains almost constant.

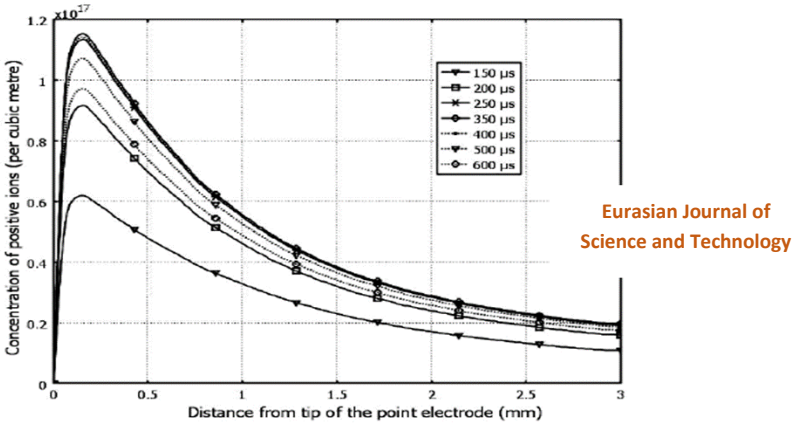

Figure 5 Positive ion density at air distance with 5kv switching

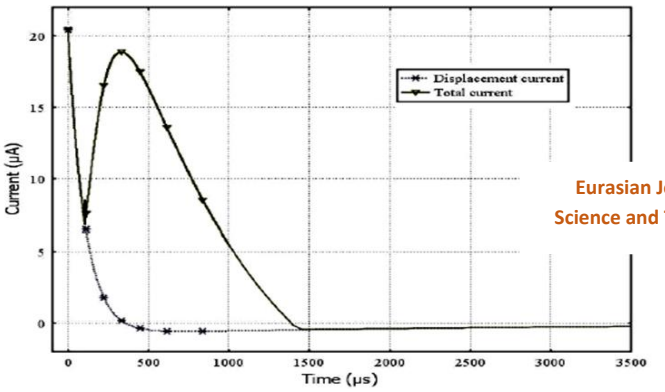

Figure 6 Circuit output current calculated for 5kv switching shock

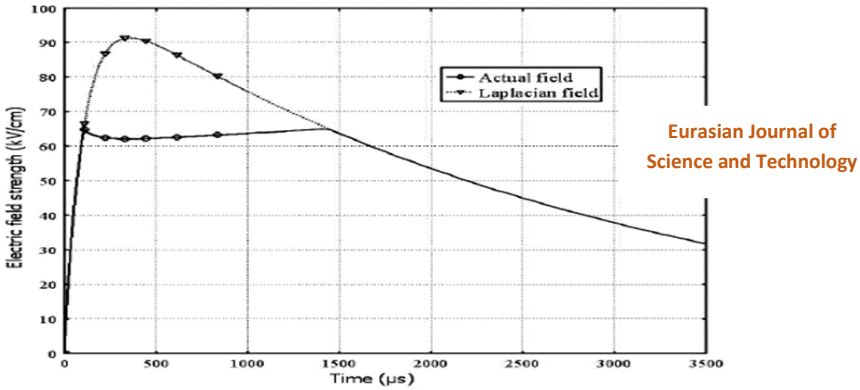

Figure 7 Real and Laplace electric field intensities at the tip of the needle electrode with 5kv switching pulse

Burst Impulse Corona

The density distribution of positive ions over an air gap over a short period of time is shown in Figure 8. This indicates that the concentration of positive ions decreases with increasing distance from the tip of the needle electrode. Figure 9 shows the formation and release of positive charge during burst pulses. The electric charge forms near the electrode anode and is concentrated for a short time (t = 12.03μs, t = 12.05μs). And as we move towards the cathode, the intensity of the field decreases and the density of ions decreases in time (t = 12.09-12.30μs). Explosive pulses seem to oppose the Laplace field due to the high density generated in the charging space generated in its own field. Figure 10 shows the decrease in electric field strength on the surface of the corona electrode and the decrease in ionization intensity. Figure 11 shows the current calculated for the 5kv shock.

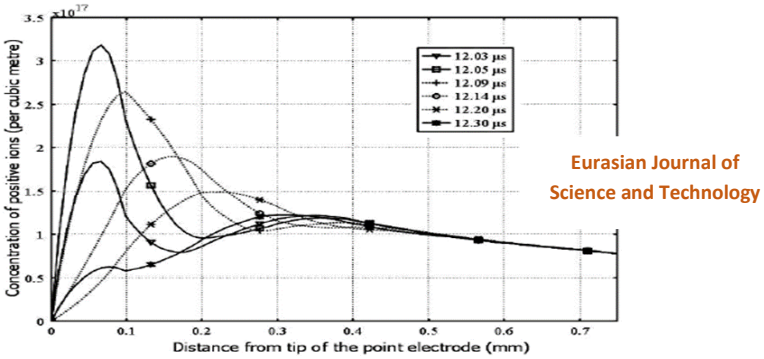

Figure 8 Positive ion density in air gap with 5kv impact

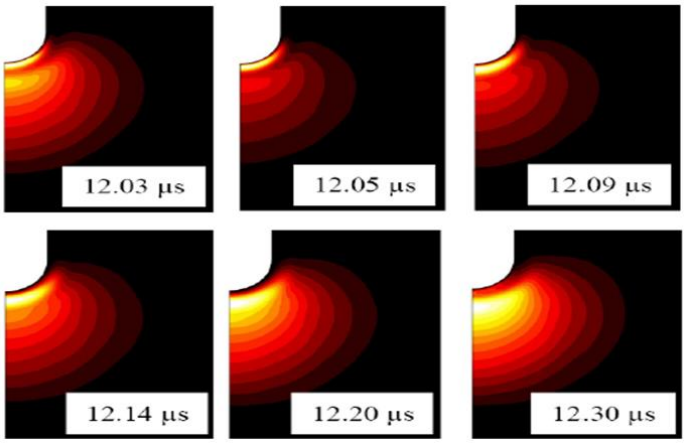

Figure 9 Changes and propagation of positive ions in the burst pulse

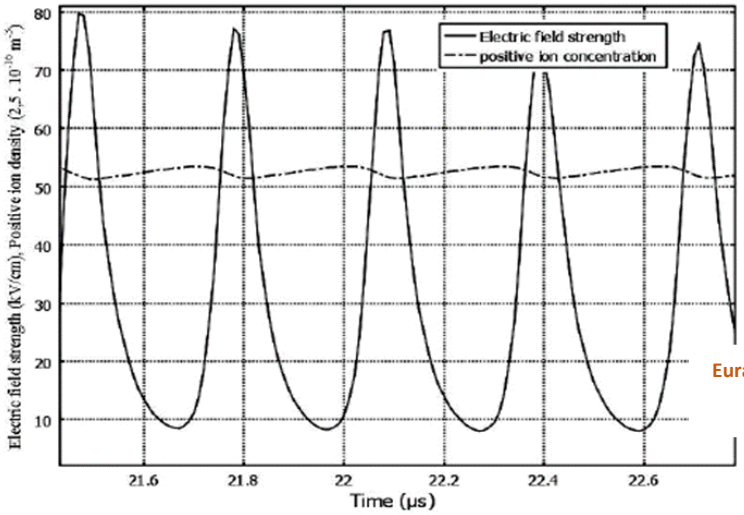

Figure 10 The difference between the electric field and the density of positive ions at a point close to the needle electrode

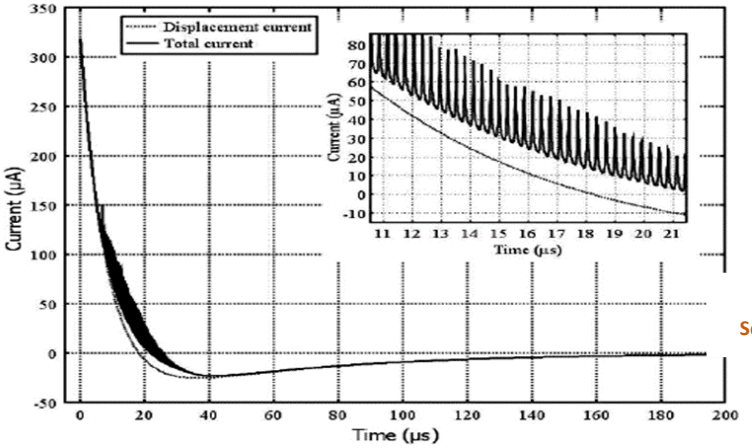

Figure 11 Current calculated with 5kv shock

Conclusion

In this paper, the intensity of the electric field with a 6kv switching impact on a resistive material is shown. The field strength increases in the vicinity of the needle electrode, and the field strength reaches the ionization threshold at 60 ° C, after which the corona threshold begins. The electrical discharge of the corona starts at 1500 μ t burst pulses appear to oppose Laplace field due to the high density generated in the charging space generated in its own field. The results in this paper showed that in the glow corona, electric charge is observed continuously and the radius of the charged point on the integrated surface gradually increases. But in a burst corona, a series of ions are released from the solid gas, which is generally less than the radiated charge in the burst corona.

ORCID

Ebadollah Amouzad Mahdiraji
https://orcid.org/0000-0003-3777-4811

References

[1] E.A. Mahdiraji, M.S. Amiri, *J. Sci. Tech. Res.*, **2021**, *1*, 89-103. **[crossref], [Google Scholar], [Publisher]**
[2] E.A. Mahdiraji, M.S. Amiri, *J. Sci. Tech. Res.*, **2021**, *1*, 11-19. **[crossref], [Google Scholar], [Publisher]**
[3] E.A. Mahdiraji, *J. Sci. Tech. Res.*, **2021**, *1*, 40-47. **[crossref], [Google Scholar], [Publisher]**
[4] E.A. Mahdiraji, R. Kolbadinezhad, *J. Sci. Tech. Res.*, **2021**, *1*, 142-149. **[crossref], [Google Scholar], [Publisher]**
[5] E.A. Mahdiraji, R. Kolbadinezhad, *J. Sci. Tech. Res.*, **2021**, *1*, 131-141. **[crossref], [Google Scholar], [Publisher]**
[6] E.A. Mahdiraji, *J. Sci. Tech. Res.*, **2021**, *1*, 75-82. **[crossref], [Google Scholar], [Publisher]**
[7] E.A. Mahdiraji, *J. Eng. Indu. Res.*, **2021**, *2*, 202-209. **[crossref], [Google Scholar], [Publisher]**
[8] E.A. Mahdiraji, *J. Eng. Indu. Res.*, **2021**, *2*, 178-193. **[crossref], [Google Scholar], [Publisher]**
[9] E.A. Mahdiraji, M.S. Amiri, *J. Eng. Indu. Res.*, **2021**, *2*, 23-31. **[crossref], [Google Scholar], [Publisher]**
[10] E.A. Mahdiraji, M.S. Amiri, *J. Eng. Indu. Res.*, **2020**, *1*, 111-122. **[crossref], [Google Scholar], [Publisher]**
[11] E.A. Mahdiraji, A.Y. Talouki, *J. Chem. Rev.*, **2021**, *3*, 348-357. **[crossref], [Google Scholar], [Publisher]**
[12] E.A. Mahdiraji, A.Y. Talouki, *J. Chem. Rev.*, **2020**, *2*, 284-291. **[crossref], [Google Scholar], [Publisher]**
[13] E.A. Mahdiraji, S.M. Shariatmadar, *Adv. J. Sci. Eng.*, **2020**, *1*, 27-31. **[crossref], [Google Scholar], [Publisher]**
[14] E.A. Mahdiraji, M.S. Amiri, *Adv. J. Sci. Eng.*, **2020**, *2*, 42–50. **[crossref], [Google Scholar], [Publisher]**
[15] E.A. Mahdiraji, N. Ramezani, *International Academic Journal of Science and Engineering*, **2016**, *3*, 1-12. **[crossref], [Google Scholar], [Publisher]**
[16] E. A. Mahdiraji, N. Ramezani, *2015 2nd International Conference on Knowledge-Based Engineering and Innovation (KBEI), Tehran, Iran*, **2015**, 405-411. **[crossref], [Google Scholar], [Publisher]**
[17] E.A. Mahdiraji, M.S. Amiri, *Journal of Engineering Technology and Applied Sciences*, **2020**, *5*, 133-147. **[crossref], [Google Scholar], [Publisher]**
[18] E.A. Mahdiraji, *Journal of Scientific Perspectives*, **2020**, *4*, 245-254. **[crossref], [Google Scholar], [Publisher]**
[19] E.A. Mahdiraji, S.M. Shariatmadar, *J. Eng. Indu. Res.*, **2021**, *2*, 210-217. **[crossref], [Google Scholar], [Publisher]**
[20] E.A. Mahdiraji, K.A. Mahdiraji, *J. Eng. Indu. Res.*, **2021**, *2*, 228-233. **[crossref], [Google Scholar], [Publisher]**
[21] E.A. Mahdiraji, *J. Chem. Rev.*, **2021**, *3*, 147-159. **[crossref], [Google Scholar], [Publisher]**
[22] H.M. Kudyan, C.H. Shih, *IEEE Trans. Power App. Syst.*, **1981**, *PAS-100*, 1420-1430. **[crossref], [Google Scholar], [Publisher]**
[23] C. De Jesus, M.T.C. de Barros, *IEEE Trans. Power Del.*, **1994**, *9*, 1564-1569. **[crossref], [Google Scholar], [Publisher]**
[24] T.H. Thang, Y. Baba, N. Nagaoka, A. Ametani, N. Itamoto, A.R. Vladimir, *IEEE*

Transaction on Electromagnetic Compatibility, **2014**, *56*, 168-176. **[crossref], [Google Scholar], [Publisher]**

[25] J. Wang, X. Wang, *2011 International Conference on Electrical and Control Engineering*, IEEE. **2011**, 696-699. **[crossref], [Google Scholar], [Publisher]**

[26] V. Cooray, N. Theethayi, *IEEE Transaction on Antenna and Propagation*, **2008**, *56*, 1948-1959 . **[crossref], [Google Scholar], [Publisher]**

[27] A.S. Mootaab, S.H. Fathi, B. Vahidi, *2009 International Conference on Electric Power and Energy Conversion Systems,(EPECS),* **2009**, 1-5 IEEE. **[crossref], [Google Scholar], [Publisher]**

[28] S. Antifeshan. A. Gholami, M. Mohajeri, Analysis of corona Effect on lightning performance of HV Overhead Transmission line using ATP/EMTP: *20TH Iranian Conference on Electrical Engineering, (ICEE 2012)*, IEEE, **2012**, 485-488. **[crossref], [Google Scholar], [Publisher]**

[29] A. Bozorgian, S. Zarinabadi, A. Samimi, *Journal of Chemical Reviews*, **2020**, *2*, 122-129. **[crossref], [Google Scholar], [Publisher]**

[30] A. Bozorgian, *Journal of Engineering in Industrial Research*, **2020**, *1*, 1-19. **[crossref], [Google Scholar], [Publisher]**

[31] N. Kayedi, A. Samimi, M. Asgari Bajgirani, A. Bozorgian, *South African Journal of Chemical Engineering*, **2021**, *35*, 153-158. **[crossref], [Google Scholar], [Publisher]**

[32] S. Kumara. Y.V. Serdyuk, S.M. Gubanski, *IEEE Transaction on Dielecterics and Electrical Insulation*, **2009**, *16*, 726-733. **[crossref], [Google Scholar], [Publisher]**

[33] H. Wei-Gang, W. Xiao-ping, *IEEE Transaction on Dielectrics and Electrical Insulation*, **1997**, *4*, 758-762. **[crossref], [Google Scholar], [Publisher]**

[34] T. Noda, T. Ono, H. Matsubara, H. Motoyama, S. Sekioka, A. Ametani, *IEEE Transaction on power Delivery*, **2003**, *18*, 307-314. **[crossref], [Google Scholar], [Publisher]**

[35] J.R. Marti, F. Castellanos, N. Santiago, *IEEE Transaction on Power Systems*, **1995**, *10*, 1003-1013. **[crossref], [Google Scholar], [Publisher]**

[36] S. Carneiro, J.R. Marti, *IEEE Transaction on Power Delivery*, **1991**, *6*, 334-342. **[crossref], [Google Scholar], [Publisher]**

[37] S.M.S. Mirnezami, F. Zare Kazemabadi, A. Heydarinasab, *Progress in Chemical and Biochemical Research*, **2021**, *4*, 191-206. **[crossref], [Google Scholar], [Publisher]**

[38] F. Zare Kazemabadi, A. Heydarinasab, A. Akbarzadehkhiyavi, M. Ardjmand, Chemical Methodologies, **2021**, *5*, 135-152. **[crossref], [Google Scholar], [Publisher]**

[39] F. Zare Kazemabadi, A. Heydarinasab, A. Akbarzadeh, M. Ardjmand, *Artificial cells, nanomedicine, and biotechnology*, **2019**, *47*, 3222-3230. **[crossref], [Google Scholar], [Publisher]**

[40] C.E.R. Bruce, R.H. Golde, 'The lightning discharge'. *J. Inst. Elec. Eng.*, 1941, 88, 487–520. **[crossref], [Google Scholar], [Publisher]**

[41] A. Bozorgian, *Journal of Engineering in Industrial Research*, **2021**, *2*, 90-94. **[crossref], [Google Scholar], [Publisher]**